This is a preprint, the final version is subject to change, of the American Mineralogist (MSA)
Cite as Authors (Year) Title. American Mineralogist, in press.
(DOI will not work until issue is live.) DOI: http://dx.doi.org/10.2138/am.2013.4243

REVISION 1

Oxy-vanadium-dravite, $NaV_3(V_4Mg_2)(Si_6O_{18})(BO_3)_3(OH)_3O$: crystal structure and redefinition of the "vanadium-dravite" tourmaline

FERDINANDO BOSI[1], LEONID Z. REZNITSKII[2] AND EUGENE V. SKLYAROV[2]

[1] Dipartimento di Scienze della Terra, Sapienza Università di Roma, P.le A. Moro, 5, I-00185 Rome, Italy
[2] The Siberian Division of Russian Academy of Sciences, Institute of the Earth's Crust, Irkutsk, 664033 Russia

ABSTRACT

"Vanadium-dravite" $NaMg_3V_6(Si_6O_{18})(BO_3)_3(OH)_3OH$ (IMA number 1999-050) has been redefined as oxy-vanadium-dravite with end-member formula $NaV_3(V_4Mg_2)Si_6O_{18}(BO_3)_3(OH)_3O$. The new name and the new formula have been approved by the CNMNC (IMA proposal 11-E). Oxy-vanadium-dravite occurs in the metamorphic rocks of the Sludyanka complex (southern Baikal region, Russia). The crystal structure of oxy-vanadium-dravite has been refined for the first time using single-crystal X-ray data, with a statistical index $R1$ for all reflections converging to 1.44%. The structure is rhombohedral, space group $R3m$, with the unit-cell parameters a = 16.1908(4), c = 7.4143(2) Å, V = 1683.21(7) Å^3, Z = 3. The chemical characterization resulted in the empirical structural formula:

$^{X}(Na_{0.88}K_{0.07}\square_{0.05})\ ^{Y}(V^{3+}_{2.46}Mg_{0.48}Ti_{0.06})\ ^{Z}(V^{3+}_{3.14}Mg_{1.74}Al_{0.91}Cr^{3+}_{0.21})\ ^{T}(Si_{5.99}Al_{0.01}O_{18})\ ^{B}(BO_3)_3\ ^{V}(OH)_3\ ^{W}(O_{0.78}OH_{0.14}F_{0.08})$.

Ideally, the oxy-vanadium-dravite is related to oxy-dravite and oxy-chromium-dravite by the homovalent substitution $V^{3+} \rightarrow Al$ and $V^{3+} \rightarrow Cr^{3+}$ (respectively) at the Y and Z sites. The occurrence of solid-solutions among V^{3+}, Cr^{3+} and Al have been observed in tourmalines from metamorphic rocks of the Sludyanka complex. Significant chemical variations in V^{3+}, Cr^{3+} and Al were also observed within zoned crystals from Sludyanka, not belonging to the holotype specimen.

INTRODUCTION

The tourmaline-supergroup minerals are the most widespread complex borocyclosilicate minerals and very useful for understanding crustal evolution (e.g., Novák et al. 2004; Agrosì et al. 2006; Lussier et al. 2011a; Novák et al. 2011; Van Hinsberg et al. 2011). The crystal structure and crystal chemistry of tourmaline have been widely studied (e.g., Foit 1989; Hawthorne 1996, 2002; Hawthorne and Henry 1999; Bosi and Lucchesi 2007; Lussier et al. 2008, 2009; van Hinsberg and Schumacher 2009; Bosi 2010, 2011; Bosi et al. 2010; Lussier et al. 2011b). The general formula of tourmaline may be formalized as $XY_3Z_6T_6O_{18}(BO_3)_3V_3W$. Henry et al. (2011) suggested the following site occupancies: $^{[9]}X$ = Na^+, K^+, Ca^{2+}, □ (=vacancy); $^{[6]}Y$ = Al^{3+}, Fe^{3+}, Cr^{3+}, V^{3+}, Mg^{2+}, Fe^{2+}, Mn^{2+}, Zn, Ni^{2+}, Co^{2+}, Cu^{2+}, Li, Ti^{4+}; $^{[6]}Z$ = Al^{3+}, Fe^{3+}, Cr^{3+}, V^{3+}, Mg^{2+}, Fe^{2+}; $^{[4]}T$ = Si^{4+}, Al^{3+}, B^{3+}; $^{[3]}B$ = B; $^{[3]}V$ (≡O3) = OH^{1-}, O^{2-}; $^{[3]}W$ (≡ O1) = OH^{1-}, F^{1-}, O^{2-}. The dominance of these ions at one or more sites of the structure gives rise to many distinct mineral species (Henry et al. 2011).

In this paper we describe the crystal structure and ideal formula of oxy-vanadium-dravite, the new name given to the former "vanadium-dravite". Tourmaline with predominance of V^{3+} among R^{3+}-cations (= Cr + V + Al) was found in Cr^{3+}-V^{3+}-bearing metamorphic rocks of the Sludyanka complex (southern Baikal region, Russia) and approved by the Commission on New Minerals, Nomenclature and Classification (CNMNC) of the International Mineralogical Association (IMA) under the name “vanadiumdravite” (IMA 1999-050), after modified as “vanadium-dravite” by Henry et al. (2011). However, in that time, as no distinction was done for the *V* and *W* anion sites of the “vanadium-dravite”, the OH group was assumed to be the dominant anion at the two OH-bearing sites combined into a single site (*V* + *W*). In addition, because of lack of crystal structure information, the cation distribution over *Y*- and *Z*-sites was not determined and an ideal end-member formula $NaMg_3V_6(Si_6O_{18})(BO_3)_3(OH)_4$ was thus assumed (Reznitsky et al. 2001). The name “vanadium-dravite” was therefore given for its relationship to dravite via the substitution Al → V^{3+}. However, Reznitsky et al. (2001) mentioned also that the sum of R^{3+}-cations, calculated with the assumption (*T* + *Y* + *Z*) = 15, in the “vanadium-dravite” is always above 6 atoms per formula unit (apfu), Mg lower than 3 apfu, and calculated OH lower than 3.5 apfu at insignificant concentrations of F. From that data, it can now be deduced that the original “vanadium-dravite” composition belongs to oxy-tourmalines (e.g., Henry et al. 2011). Thus, we have conducted X-ray single-crystal investigation on the original “vanadium-dravite” from the type locality. For the study, the microcrystal labeled as 8-25, which is part of the holotype

material of the original "vanadium-dravite", was chosen. The new name and new end-member formula have been approved by the IMA-CNMNC, proposal 11-E.

EXPERIMENTAL METHODS

Single-crystal structural refinement

A representative crystal of the type specimen was selected for X-ray diffraction measurements on a Bruker KAPPA APEX-II single-crystal diffractometer, at Sapienza University of Rome (Earth Sciences Department), equipped with CCD area detector (6.2 × 6.2 cm^2 active detection area, 512 × 512 pixels) and a graphite crystal monochromator, using Mo$K\alpha$ radiation from a fine-focus sealed X-ray tube. The sample-to-detector distance was 4 cm. A total of 4007 exposures (step = 0.2°, time/step = 20 s) covering a full reciprocal sphere with a high redundancy of about 7 were used. Final unit-cell parameters were refined by means of the Bruker AXS SAINT program using reflections with $I > 10\ \sigma(I)$ in the range $6° < 2\theta < 82°$. The intensity data were processed and corrected for Lorentz, polarization, and background effects with the APEX2 software program of Bruker AXS. The data were corrected for absorption using the multi-scan method (SADABS). The absorption correction led to a significant improvement in R_{int}. No violations of $R3m$ symmetry were noted.

Structural refinement was carried out with the SHELXL-97 program (Sheldrick 2008). Starting coordinates were taken from Bosi (2008). Variable parameters were: scale factor, extinction coefficient, atomic coordinates, site scattering values expressed as mean atomic number (for *X*, *Y*, and *Z* sites) and atomic displacement factors. To obtain the best values of statistical indexes ($R1$, $wR2$), fully ionized V and O scattering curves were used, whereas neutral scattering curves were used for the other atoms. In detail, the *X* and *Y* sites were modeled using Na and V scattering factors, respectively. The occupancy of the *Z* was obtained considering the presence of V vs. Mg. The *T* and *B* sites were modeled, respectively, with Si and B scattering factors and with a fixed occupancy of 1, because refinement with unconstrained occupancies showed no significant deviations from this value. Three full-matrix refinement cycles with isotropic displacement parameters for all atoms were followed by anisotropic cycles until convergence was attained. No correlations over a value of 0.7 between the parameters were observed at the end of refinement. Table 1 lists crystal data, data collection information and refinement details; Table 2 gives the fractional atomic coordinates and site occupancies; Table 3 gives the displacement parameters; Table 4 gives selected bond distances.

Electron microprobe analysis

Electron microprobe analyses by wavelength dispersive spectroscopy of the crystal used for structural studies were obtained with a Cameca SX50 instrument at the "Istituto di Geologia Ambientale e Geoingegneria (CNR of Rome, Italy)", operating at an accelerating potential of 15 kV and a sample current of 15 nA (10 μm beam diameter). Minerals and synthetic compounds were used as standards: wollastonite (Si, Ca), magnetite (Fe), rutile (Ti), corundum (Al), fluor-phlogopite (F), periclase (Mg), jadeite (Na), K-feldspar (K), sphalerite (Zn), metallic Cr, V, Mn and Cu. V and Cr concentrations were corrected for interference from the Ti-*K*β and V-*K*β peaks, respectively. The PAP matrix correction procedure (Pouchou and Pichoir 1991) was applied to reduce the raw data. The results, which are summarized in Table 5, represent mean values of 8 spots. In accordance with the documented very low concentration of Li in dravitic samples (e.g., Henry et al. 2011), the Li_2O content was assumed to be insignificant. FeO, MnO, ZnO, CuO, and CaO were not detected with their concentrations being below the minimum detection limits (0.03 wt%).

Other properties such as X-ray powder diffraction data and physical properties of the mineral are reported in Reznitsky et al. (2001) and Jambor et al. (2002).

RESULTS

Determination of atomic proportions

In agreement with the structural refinement results, the boron content was assumed to be stoichiometric in the oxy-vanadium-dravite (B = 3.00 apfu). In fact, both the site-scattering results and the bond lengths of *B* and *T* are consistent with both the *B* site fully occupied by boron, and no B at the *T* site. The OH content can then be calculated by charge balance with the assumption ($T + Y + Z$) = 15.00. The atomic proportions were calculated on this assumption (Table 5). The excellent match between the number of electrons per formula unit (epfu) derived from chemical and structural analysis supports this procedure: 268.72 epfu and 268.70 epfu, respectively

Determination of site populations

The site allocation of anions in the studied sample followed the general preference suggested for tourmaline (e.g., Grice and Ercit 1993; Henry et al. 2011): the O3 site (*V* position in the general formula) is occupied by OH, while the O1 site (*W* position in the

general formula) can be occupied by O^{2-}, OH^{1-} and F^{1-}. The cation distribution at the *T*, *Y* and *Z* sites was optimized by using a quadratic program to minimize the residuals between calculated and observed data (based on the chemical and structural analysis). Site scattering values, octahedral and tetrahedral mean bond distances (i.e., <*Y*-O>, <*Z*-O> and <*T*-O>) were calculated as the linear contribution of each cation multiplied by its specific bond distance (Table 6). More details about the specific distances as well as about the optimization procedure may be found in Bosi et al. (2004). The robustness of this approach was confirmed by another optimization procedure (Wright et al. 2000), which led to very similar cation distributions (Table 6). This result represents another example of convergence of these two procedures to similar solutions for tourmaline (e.g., Bosi and Lucchesi 2007; Filip et al. 2012). The final structural formula is as follows:

$^{X}(Na_{0.88}K_{0.07}\square_{0.05})\ ^{Y}(V^{3+}_{2.46}Mg_{0.48}Ti_{0.06})\ ^{Z}(V^{3+}_{3.14}Mg_{1.74}Al_{0.91}Cr^{3+}_{0.21})\ ^{T}(Si_{5.99}Al_{0.01}O_{18})\ ^{B}(BO_3)_3$
$^{V}(OH)_3\ ^{W}(O_{0.78}OH_{0.14}F_{0.08})$

The bond-valence analysis is also consistent with the proposed structural formula. Bond valence calculations, using the formula and bond-valence parameters from Brown and Altermatt (1985), are reported in Table 7.

DISCUSSION

The new chemical analytical data are very close (statically identical) to the one presented by Reznitsky et al. (2001), showing that chemical variations between individual crystals of (oxy-)vanadium-dravite of the holotype material are practically insignificant. The low standard deviations of the measured elements (Table 5) demonstrate the chemical homogeneity of the representative crystal (sample 8-25).

The composition of the present sample is consistent with a tourmaline belonging to the alkali group, oxy-subgroup 3 (Henry et al. 2011): Na-dominant at the *X* position of the general formula, $O^{2-} > (OH^{1-}+F^{1-})$ at the *W* position, V^{3+} is the dominant trivalent cation at *Y* and *Z*, and Mg is the dominant divalent cation at *Z* (Fig 1). The ideal end-member may therefore be represented as $NaV_3(V_4Mg_2)Si_6O_{18}(BO_3)_3(OH)_3O$. In accordance with these results, the original name "vanadium-dravite", while still reflecting its relationship to dravite, does not take into account the fact that O^{2-} is dominant at the *W* position. By analogy with the relation between dravite and oxy-dravite (IMA 2012-004a) as well as between chromium-dravite and oxy-chromium-dravite (IMA 2011-097; Bosi et al. 2012), this end-member species has been given the name oxy-vanadium-dravite. In line with the above-mentioned oxy-transitions, the

prefix *oxy* represents the heterovalent substitution $V^{3+} + O^{2-} \rightarrow Mg^{2+} + OH^{1-}$ relative to the root composition "vanadium-dravite" (Table 8).

Ideally, oxy-vanadium-dravite is related to oxy-dravite and oxy-chromium-dravite by the homovalent substitutions $V^{3+} \rightarrow Al$ and $V^{3+} \rightarrow Cr^{3+}$ (respectively) at the *Y* and *Z* sites. The triangular plot in terms of Al^{3+}-V^{3+}-Cr^{3+} at (*Y* + *Z*) shows the wide compositional range of V^{3+}-dominant tourmalines from Sludyanka as well as the position of V^{3+}-bearing oxy-chromium-dravite samples and V^{3+}-bearing oxy-dravite from the literature (Fig. 1). The occurrence of solid solutions among V^{3+}, Cr^{3+} and Al have been observed by chemical analyses of several tourmalines from metamorphic rocks of the Sludyanka complex (Fig 2) as well as in the study of Reznitsky et al. (2001). All of these tourmalines are characterized by negligible Fe concentrations. Figure 3 shows that significant chemical variations in V^{3+}, Cr^{3+} and Al contents occur not only between different tourmaline crystals of a rock sample but also within the same non-homogeneous crystal, which does not belong to the holotype specimen.

ACKNOWLEDGMENTS

Chemical analyses were carried out with the kind assistance of M. Serracino to whom the authors express their gratitude. Comments and suggestions by the AE Fernando Colombo, Federico Pezzotta and Marian Lupulescu are very appreciated.

REFERENCES

Agrosì, G., Bos,I F., Lucchesi, S., Melchiorre, G., and Scandale, E. (2006) Mn-tourmaline crystals from island of Elba (Italy): growth history and growth marks. American Mineralogist, 91, 944-952.

Bosi, F. (2008) Disordering of Fe^{2+} over octahedrally coordinated sites of tourmaline. American Mineralogist, 93, 1647-1653.

Bosi, F. (2010) Octahedrally coordinated vacancies in tourmaline: a theoretical approach. Mineralogical Magazine, 74, 1037-1044.

Bosi, F. (2011) Stereochemical constraints in tourmaline: from a short-range to a long-range structure. Canadian Mineralogist, 49, 17-27.

Bosi, F. and Lucchesi, S. (2007) Crystal chemical relationships in the tourmaline group: structural constraints on chemical variability. American Mineralogist, 92, 1054-1063.

198 Bosi F., Lucchesi S., and Reznitskii L. (2004) Crystal chemistry of the dravite-chromdravite
199 series. European Journal of Mineralogy, 16, 345-352.
200 Bosi, F., Reznitskii, L. and Skogby, H. (2012) Oxy-chromium-dravite,
201 $NaCr_3(Cr_4Mg_2)(Si_6O_{18})(BO_3)_3(OH)_3O$, a new mineral species of the tourmaline
202 supergroup. American Mineralogist, doi: 10.2138/am.2012.4210.
203 Bosi, F., Agrosì, G., Lucchesi, S., Melchiorre G., and Scandale, E. (2005a) Mn-tourmaline
204 from island of Elba (Italy). Crystal chemistry. American Mineralogist, 90, 1661-1668.
205 Bosi, F., Andreozzi G.B., Federico M., Graziani G., and Lucchesi S. (2005b) Crystal
206 chemistry of the elbaite-schorl series. American Mineralogist, 90, 1784-1792.
207 Bosi, F., Balić-Žunić, T., and Surour, A.A. (2010) Crystal structure analysis of four
208 tourmalines from the Cleopatra's Mines (Egypt) and Jabal Zalm (Saudi Arabia), and the
209 role of Al in the tourmaline group. American Mineralogist, 95, 510-518.
210 Brown, I.D. and Altermatt, D. (1985) Bond-valence parameters obtained from a systematic
211 analysis of the Inorganic Crystal Structure Database. Acta Crystallographica, B41, 244-
212 247.
213 Filip, J., Bosi, F., Novák, M., Skogby, H., Tuček, J., Čuda, J., and Wildner, M. (2012) Redox
214 processes of iron in the tourmaline structure: example of the high-temperature treatment
215 of Fe^{3+}-rich schorl. Geochimica et Cosmochimica Acta, 86, 239-256.
216 Foit, F.F. Jr. (1989) Crystal chemistry of alkali-deficient schorl and tourmaline structural
217 relationships. American Mineralogist, 74, 422-431.
218 Foit, F.F. and Rosenberg, P.F. (1979) The structure of vanadium-bearing tourmaline and its
219 implications regarding tourmaline solid solutions. American Mineralogist, 64, 788.798.
220 Grice, J.D. and Ercit, T.S. (1993) Ordering of Fe and Mg in the tourmaline crystal structure:
221 the correct formula. Neues Jahrbuch für Mineralogie, Abhandlungen, 165, 245-266.
222 Hawthorne, F.C. (1996) Structural mechanisms for light-element variations in tourmaline.
223 Canadian Mineralogist, 34, 123-132.
224 Hawthorne, F. C. (2002) Bond-valence constraints on the chemical composition of tourmaline.
225 Canadian Mineralogist, 40, 789–797.
226 Hawthorne, F.C. and Henry, D. (1999) Classification of the minerals of the tourmaline group.
227 European Journal of Mineralogy, 11, 201-215.

Henry, D.J., Novák, M., Hawthorne, F.C., Ertl, A., Dutrow, B., Uher, P., and Pezzotta, F. (2011) Nomen□loture of the tourmaline-supergroup minerals. American Mineralogist, 96, 895-913.

Jambor, J.L., Grew, E.S. and Roberts, A.C. (2002) New mineral names. American Mineralogist, 87, 1509-1513.

Lussier, A.J., Aguiar, P.M., Michaelis, V.K., Kroeker, S., Herwig, S., Abdu, Y., and Hawthorne, F.C. (2008) Mushroom elbaite from the Kat Chay mine, Momeik, near Mogok, Myanmar: I. Crystal chemistry by SREF, EMPA, MAS NMR and Mössbauer spectroscopy. Mineralogical Magazine, 72, 747-761.

Lussier, A.J., Aguiar, P., Michaelis, V., Kroeker, S., and Hawthorne, F.C. (2009) The occurrence of tetrahedrally coordinated Al and B in tourmaline: An ^{11}B and ^{27}Al MAS NMR study. American Mineralogist, 94, 785-792.

Lussier A. J., Hawthorne F. C., Aguiar P. M., Michaelis V. K., and Kroeker S. (2011a) Elbaite-liddicoatite from Black Rapids glacier, Alaska. Periodico di Mineralogia, 80, 57–73.

Lussier, A.J., Abdu, Y. Hawthorne, F.C., Michaelis, V.K., Aguiar, P.M., and Kroeker, S. (2011b) Oscillatory zoned liddicoatite from Anjanabonoina, central Madagascar. I. Crystal chemistry and structure by SREF and ^{11}B and ^{27}Al MAS NMR spectroscopy. Canadian Mineralogist, 49, 63-88.

Novák, M., Povondra, P., and Selway, J.B. (2004) Schorl-oxy-schorl to dravite-oxy-dravite tourmaline from granitic pegmatites; examples from the Moldanubicum, Czech Republic. European Journal of Mineralogy, 16, 323-333.

Novák M., Škoda P., Filip J., Macek I., and Vaculovič T. (2011) Compositional trends in tourmaline from intragranitic NYF pegmatites of the Třebíč Pluton, Czech Republic: an electron microprobe, Mössbauer and LA-ICP-MS study. Canadian Mineralogist, 49, 359-380.

Pouchou, J.L. and Pichoir, F. (1991) Quantitative analysis of homogeneous or stratified microvolumes applying the model "PAP." In K.F.J. Heinrich and D.E. Newbury, Eds., Electron probe quantitation, p. 31-75. Plenum, New York.

Reznitsky, L.Z., Sklyarov, E.V., Ushchapovskaya, Z.V., Nartova, N.V., Kashaev, A.A., Karmanov, N.S., Kanakin, S.V., Smolin, A.S., and Nekrosova, E.A. (2001) Vanadiumdravite, $NaMg_3V_6[Si_6O_{18}][BO_3]_3(OH)_4$, a new mineral of the tourmaline

group. Zapiski Vsesoyuznogo Mineralogicheskogo Obshchestva, 130, 59-72 (in Russian).

Sheldrick, G.M. (2008) A short history of SHELX. Acta Crystallographica, A64, 112-122.

Van Hinsberg, V.J. and Schumacher, J.C. (2009) The geothermobarometric potential of tourmaline, based on experimental and natural data. American Mineralogist, 94, 761-770.

Van Hinsberg, V.J., Henry, D.J., and Marschall, H.R. (2011) Tourmaline: an ideal indicator of its host environment. Canadian Mineralogist, 49, 1-16.

Wright, S.E., Foley, J.A., and Hughes, J.M. (2000) Optimization of site occupancies in minerals using quadratic programming. American Mineralogist, 85, 524-531.

LIST OF TABLES

LIST OF FIGURES AND FIGURE CAPTIONS

FIGURE 1. Al^{3+}-V^{3+}-Cr^{3+} ternary diagram for oxy-tourmaline. Black crosses = V^{3+} dominant tourmalines from Sludyanka (ca. 160 data); black circle = studied sample (8-25); black triangles = oxy-chromium-dravite (Bosi et al. 2012); black star = oxy-dravite (Foit and Rosenberg 1979).

FIGURE 2. Plot of (Cr+V) against Al (cations) for oxy-tourmalines from Sludyanka showing the occurrence of an inverse correlation between (Cr+V) and Al.

FIGURE 3. X-ray distribution maps of Al, V, Cr in zoned crystal of V-Cr-Al tourmaline (size 50 by 200 μm), not belonging to the holotype specimen. Profiles (wt.%) for Al_2O_3, Cr_2O_3, MgO and V_2O_3 built up from A to B by a set of point analyses separated by 5 μm.

TABLE 1. Single crystal X-ray diffraction data details for oxy-vanadium-dravite

Sample 8-25	
Crystal size (mm)	$0.10 \times 0.11 \times 0.12$
a (Å)	16.1908(4)
c (Å)	7.4143(2)
V (Å^3)	1683.21(7)
Density (g/cm^3)	3.213
Range for data collection, θ (°)	2.52 - 41.03
Reciprocal space range *hkl*	$-29 \le h \le 29$
	$-29 \le k \le 24$
	$-13 \le l \le 13$
Total number of frames	4007
Set of measured reflections	9144
Unique reflections, R_{int} (%)	2242, 1.81
Absorption correction method	Multiscan
Refinement method	Full-matrix last-squares on F^2
Structural refinement program	SHELXL-97
Extinction coefficient	0.00022(9)
Flack parameter	0.087(9)
*wR*2 (%)	3.52
*R*1 (%) all data	1.44
*R*1 (%) for $I > 2\sigma_I$	1.40
GooF	1.044
Diff. Peaks ($\pm e^-$/Å^3)	0.74 and –0.32

Notes: $R_{int.}$ = merging residual value; *R*1 = discrepancy index, calculated from *F*-data; *wR*2 = weighted discrepancy index, calculated from F^2-data; GooF = goodness of fit; Diff. Peaks = maximum and minimum residual electron density. Radiation, Mo*K*α = 0.71073 Å. Data collection temperature = 293 K. Space group *R*3*m*; *Z* = 3 formula units.

TABLE 2. Fractional atomic coordinates (*x*,*y*,*z*) and site occupancies for oxy-vanadium-dravite

Sample 8-25				
Site	*x*	*y*	*z*	Site occupancy
X	0	0	0.22575(16)	$Na_{1.029(6)}$
Y	0.122910(14)	0.061455(7)	0.63907(4)	$V_{0.925(2)}$
Z	0.298218(11)	0.261727(12)	0.61043(4)	$V_{0.569(3)}Mg_{0.431(3)}$
B	0.10951(4)	0.21901(9)	0.45484(17)	$B_{1.00}$
T	0.189382(15)	0.187781(15)	0	$Si_{1.00}$
O1 (*W*)	0	0	0.76587(19)	$O_{1.00}$
O2	0.06071(3)	0.12141(6)	0.48914(12)	$O_{1.00}$
O3 (*V*)	0.25659(6)	0.12830(3)	0.50995(12)	$O_{1.00}$
O4	0.09213(3)	0.18426(7)	0.06973(12)	$O_{1.00}$
O5	0.18214(7)	0.09107(3)	0.08701(11)	$O_{1.00}$
O6	0.19183(4)	0.18285(4)	0.78271(9)	$O_{1.00}$
O7	0.28151(4)	0.28147(4)	0.07441(8)	$O_{1.00}$
O8	0.20666(4)	0.26751(4)	0.43882(9)	$O_{1.00}$
H3	0.2643(15)	0.1321(8)	0.386(3)	$H_{1.00}$

TABLE 3. Displacement parameters (Å^2) for oxy-vanadium-dravite

Sample 8-25							
Site	U^{11}	U^{22}	U^{33}	U^{23}	U^{13}	U^{12}	U_{eq}
X	0.0255(4)	0.0255(4)	0.0244(6)	0	0	0.0128(2)	0.0252(3)
Y	0.0073(1)	0.0067(1)	0.0102(1)	-0.0005(1)	-0.0010(1)	0.0036(1)	0.00800(5)
Z	0.0059(1)	0.0065(1)	0.0075(1)	0.0005(1)	0.00002(4)	0.0030(1)	0.00670(5)
B	0.0074(3)	0.0086(4)	0.0111(4)	0.0015(3)	0.0007(2)	0.0043(2)	0.00887(18)
T	0.0064(1)	0.0059(1)	0.0088(1)	-0.0004(1)	-0.0003(1)	0.0030(1)	0.00701(5)
O1 (*W*)	0.0089(3)	0.0089(3)	0.0095(5)	0	0	0.0044(1)	0.0091(2)
O2	0.0081(2)	0.0066(3)	0.0113(3)	0.0017(2)	0.0009(1)	0.0033(1)	0.00886(13)
O3 (*V*)	0.0128(3)	0.0118(3)	0.0095(3)	0.0004(1)	0.0009(3)	0.0064(2)	0.01127(14)
O4	0.0089(2)	0.0164(4)	0.0115(3)	-0.0011(3)	-0.0005(1)	0.0082(2)	0.01145(14)
O5	0.0159(4)	0.0085(2)	0.0108(3)	0.0007(1)	0.0014(3)	0.0080(1)	0.01089(14)
O6	0.0100(2)	0.0083(2)	0.0085(2)	-0.0007(2)	-0.0004(2)	0.0044(1)	0.00902(10)
O7	0.0082(2)	0.0074(2)	0.0111(2)	-0.0014(2)	-0.0012(2)	0.0016(2)	0.00992(10)
O8	0.0056(2)	0.0098(2)	0.0176(2)	0.0038(2)	0.0010(1)	0.0033(2)	0.01122(10)
H3							0.017*

Notes: U^{ij} = anisotropic displacement parameter; U_{eq} = equivalent isotropic displacement parameters
* Isotropic displacement parameter constrained to 1.5*U*eq(O3)

TABLE 4. Selected bond distances (Å) for oxy-vanadium-dravite

Sample 8-25			
B-O2	1.3920(15)	*Y*-O1	1.9632(7)
B-O8^{A} (×2)	1.3675(9)	*Y*-O2^{B} (×2)	2.0421(6)
<*B*-O>	1.376	*Y*-O3	2.1048(9)
		Y-O6^{C} (×2)	2.0124(6)
X-O2^{B,F} (×3)	2.5907(12)	<*Y*-O>	2.029
X-O4^{B,F} (×3)	2.8307(11)		
X-O5^{B,F} (×3)	2.7532(10)	*Z*-O3	2.0543(4)
<*X*-O>	2.725	*Z*-O6	2.0075(6)
		Z-O7^{E}	1.9883(6)
T-O4	1.6310(4)	*Z*-O7^{D}	2.0296(6)
T-O5	1.6426(4)	*Z*-O8^{E}	1.9632(6)
*T**-O6	1.6145(6)	*Z*-O8	1.9909(6)
T-O7	1.6024(6)	<Z-O>	2.006
<*T*-O>	1.623		
		O3-H3	0.93(2)

Notes: Standard uncertainty in parentheses. A = ($y - x$, y, z); B = ($y - x$, $-x$, z); C = (x, $x - y$, z); D = ($y - x + 1/3$, $-x + 2/3$, $z + 2/3$); E = ($-y + 2/3$, $x - y + 1/3$, $z + 1/3$); F = ($-y$, $x - y$, z). Transformations relate coordinates to those of Table 2.

* Positioned in adjacent unit cell.

TABLE 5. Chemical composition of oxy-vanadium-dravite

Sample 8-25			
	Weight %		Apfu
SiO_2	33.05(23)	Si	5.99(6)
TiO_2	0.41(4)	Ti^{4+}	0.06(1)
B_2O_3*	9.59	B	3.00
Al_2O_3	4.30(8)	Al	0.92(2)
Cr_2O_3	1.48(26)	Cr^{3+}	0.21(4)
V_2O_3	38.56(25)	V^{3+}	5.60(6)
MgO	8.21(10)	Mg	2.22(3)
Na_2O	2.50(7)	Na	0.88(3)
K_2O	0.32(2)	K	0.07(1)
F	0.13(5)	F	0.08(3)
H_2O*	2.60	OH	3.14
O=F	–0 .06	OH+F	3.22
Total	101.10		

Notes: number of ions calculated on basis of 31 (O, OH, F). Oxide values are an average of the 8 spots (standard deviation in brackets). B_2O_3 and H_2O uncertainty assumed at 5%. Standard uncertainty for ions was calculated by error-propagation theory. *Calculated by stoichiometry

TABLE 6. Cation site populations (apfu), site scattering factors (epfu) and mean bond distances (Å) for oxy-vanadium-dravite

Site	Site population	Site scattering		Mean bond length	
		refined	calculated	refined	calculated
X	0.88 Na + 0.07 K + 0.05 □	11.32(7)	11.07		
Y	2.47 V^{3+} + 0.48 Mg + 0.06 Ti^{4+}	63.8(1)	63.7	2.029	2.029
	^{Y}(2.52 V^{3+} + 0.48 Mg + 0.01 Ti^{4+})*				
Z	3.14 V^{3+} + 0.91 Al + 0.21 Cr^{3+} + 1.74 Mg	109.6(3)	109.9	2.006	2.010
	^{Z}(3.09 V^{3+} + 0.94 Al + 0.22 Cr^{3+} + 1.75 Mg)*				
T	5.99 Si + 0.01 Al	84†	83.99	1.623	1.620
	^{T}(6.00 Si)*				
B	3 B	15†	15		

Notes: apfu = atoms per formula unit; epfu = electrons per formula unit.
* Site populations optimized by the procedure of Wright et al. (2000).
† Fixed in the final stages of refinement.

TABLE 7. Bond valence calculations (valence units) for oxy-vanadium-dravite

Site	*X*	*Y*	*Z*	*T*	*B*	Σ
O1		$0.54^{\times 3}\rightarrow$				1.62
O2	$0.13^{\times 3}\downarrow$	$0.44^{\times 2}\downarrow\rightarrow$			0.95	1.96
O3		0.37	$0.40^{\times 2}\rightarrow$			1.17
O4	$0.07^{\times 3}\downarrow$			$0.99^{\times 2}\rightarrow$		2.03
O5	$0.08^{\times 3}\downarrow$			$0.95^{\times 2}\rightarrow$		1.98
O6		$0.48^{\times 2}\downarrow$	0.45	1.03		1.96
O7			0.48	1.06		1.97
			0.43			
O8			0.47		$1.01^{\times 2}\downarrow$	1.99
			0.51			
Σ	0.84	2.75	2.74	4.02	2.97	

TABLE 8. Al-Cr-V end-members relationships.

Hydroxy end-member	Coupled substitution	*Oxy* end-member
Dravite $NaMg_3Al_6Si_6O_{18}(BO_3)_3(OH)_3OH$	$Al^{3+} + O^{2-} \rightarrow Mg^{2+} + OH^{1-}$	Oxy-dravite $NaAl_3(Al_4Mg_2)Si_6O_{18}(BO_3)_3(OH)_3O$
Chromium-dravite $NaMg_3Cr_6Si_6O_{18}(BO_3)_3(OH)_3OH$	$Cr^{3+} + O^{2-} \rightarrow Mg^{2+} + OH^{1-}$	Oxy-chromium-dravite $NaCr_3(Cr_4Mg_2)Si_6O_{18}(BO_3)_3(OH)_3O$
"Vanadium-dravite" $NaMg_3V_6Si_6O_{18}(BO_3)_3(OH)_3OH$	$V^{3+} + O^{2-} \rightarrow Mg^{2+} + OH^{1-}$	Oxy-vanadium-dravite $NaV_3(V_4Mg_2)Si_6O_{18}(BO_3)_3(OH)_3O$

Figure 1

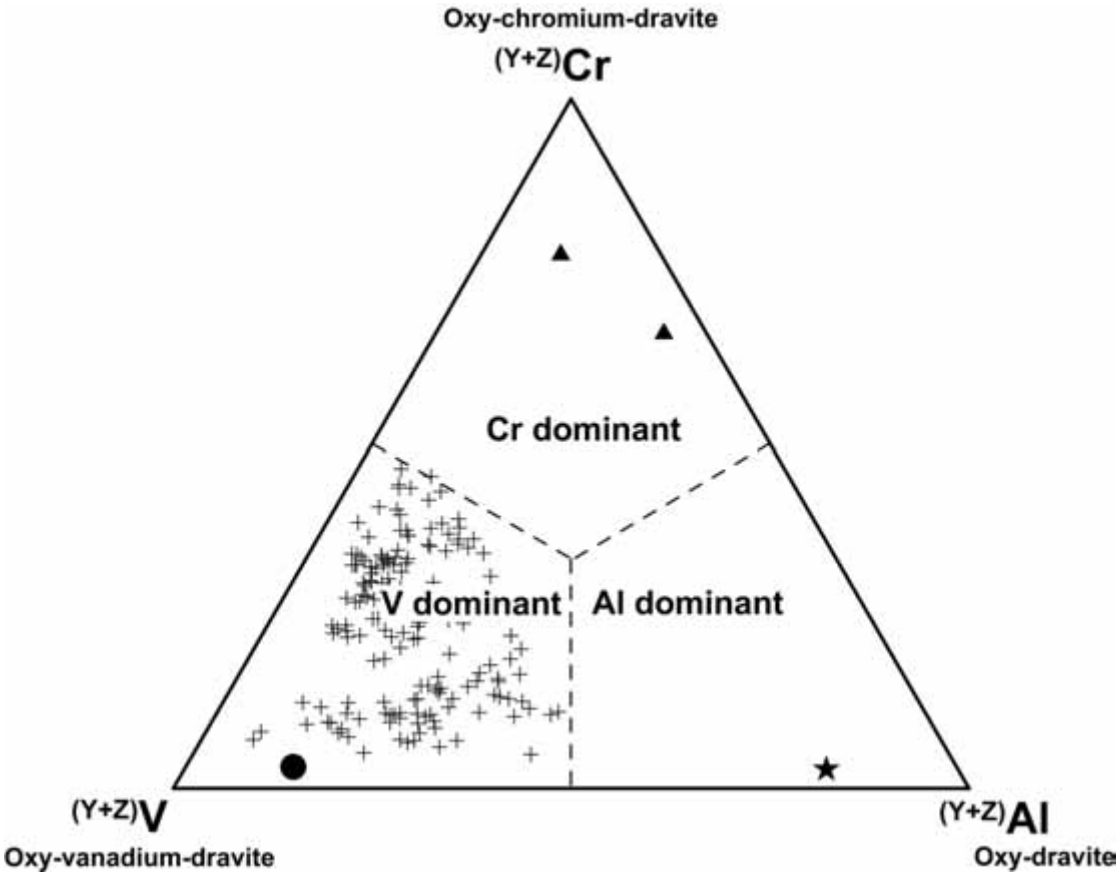
Oxy-chromium-dravite
(Y+Z)Cr
Cr dominant
V dominant
Al dominant
(Y+Z)V
Oxy-vanadium-dravite
(Y+Z)Al
Oxy-dravite

Figure 2

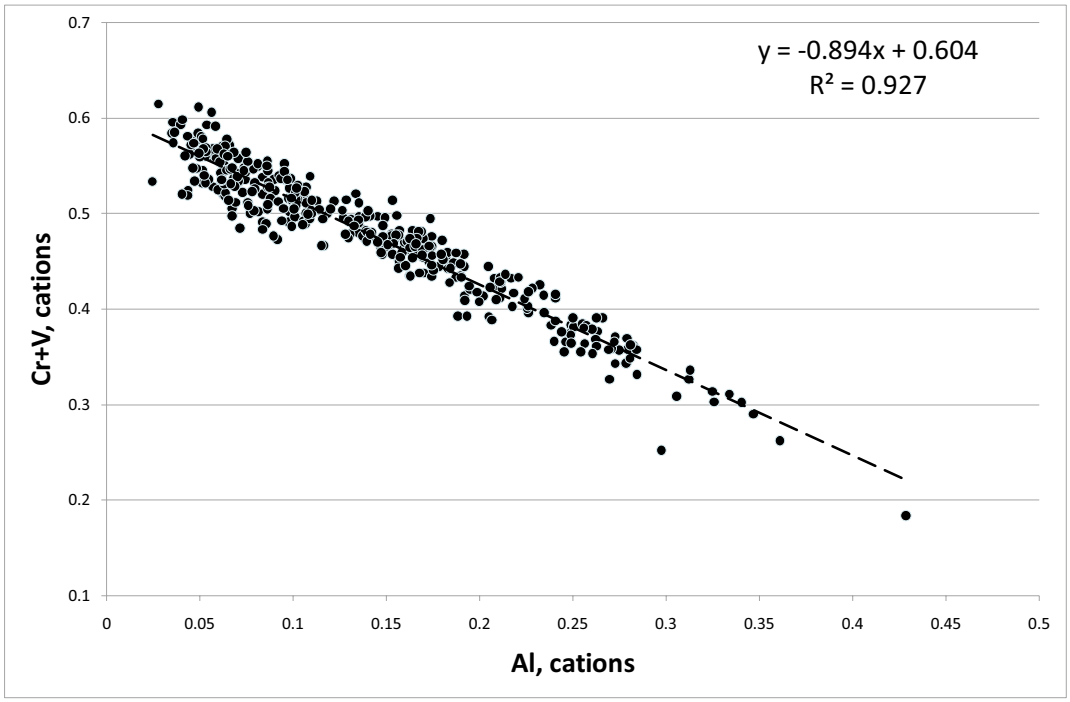
y = -0.894x + 0.604
R² = 0.927
Cr+V, cations
Al, cations
0.7
0.6
0.5
0.4
0.3
0.2
0.1
0
0.05
0.1
0.15
0.2
0.25
0.3
0.35
0.4
0.45
0.5

Figure 3

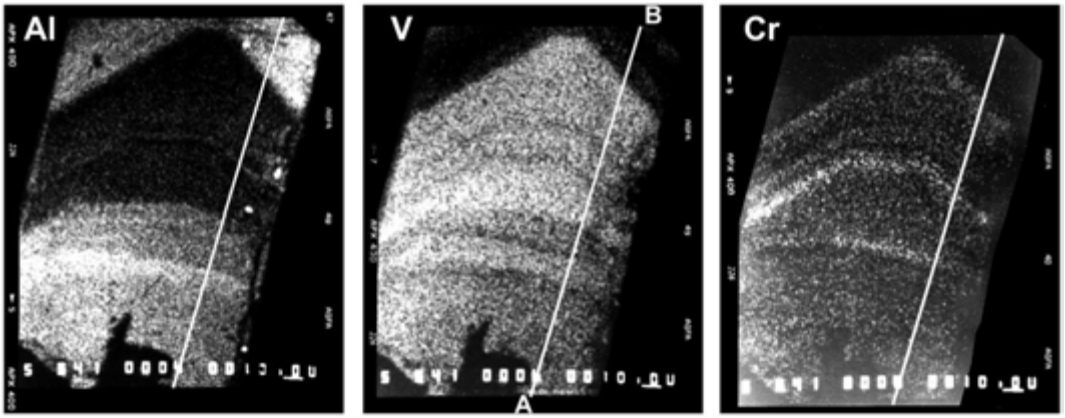
Al
V
B
A
Cr

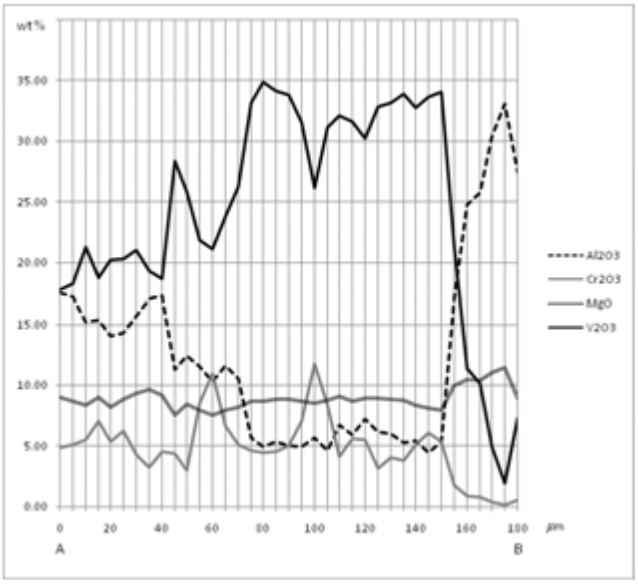
wt%
35.00
30.00
25.00
20.00
15.00
10.00
5.00
0.00
0
20
40
60
80
100
120
140
160
180
μm
A
B
Al2O3
Cr2O3
MgO
V2O3